

Spin accumulation in quantum wires with strong Rashba spin-orbit coupling

M. Governale and U. Zülicke

Institut für Theoretische Festkörperphysik, Universität Karlsruhe, D-76128 Karlsruhe, Germany

(Received 26 June 2002; published 29 August 2002)

We present analytical and numerical results for the effect of Rashba spin-orbit coupling on band structure, transport, and interaction effects in quantum wires when the spin precession length is comparable to the wire width. The situation with only the lowest spin-split subbands occupied is particularly interesting because electrons close to Fermi points of the same chirality can have approximately parallel spins. We discuss consequences for spin-dependent transport and effective Tomonaga-Luttinger descriptions of interactions in the quantum wire.

DOI: 10.1103/PhysRevB.66.073311

PACS number(s): 73.21.Hb, 71.10.Pm, 72.10.-d, 73.23.-b

Spin-dependent transport phenomena are currently attracting a lot of interest because of their potential for future electronic device applications.¹ Basic design proposals for spin-controlled field-effect switches^{2,3} use the fact that electron waves with opposite spin acquire different phase factors during their propagation in the presence of Rashba spin-orbit coupling⁴ (RSOC). The latter arises due to structural inversion asymmetry in quantum heterostructures^{5,6} where two-dimensional (2D) electron systems are realized. The single-electron Hamiltonian is then of the form⁷ $H_{2D} = H_0 + H_{so}$ where

$$H_0 = \frac{1}{2m}(p_x^2 + p_y^2), \quad (1a)$$

$$H_{so} = \frac{\hbar k_{so}}{m}(\sigma_x p_y - \sigma_y p_x), \quad (1b)$$

with m denoting the effective electron mass.²⁶ The possibility to tune the strength of the RSOC, measured here in terms of the characteristic wave vector k_{so} , by external gate voltages has been demonstrated experimentally.⁸⁻¹⁰ As a manifestation of broken spin-rotational invariance, eigenstates of H_{2D} which are labeled by a 2D wave vector \vec{k} have their spin pointing in the direction perpendicular to \vec{k} . Hence, no common spin quantization axis can be defined for eigenstates when spin-orbit coupling is present. Confining the 2D electrons further to form a quantum wire, one might naively expect to again be able to define a global spin quantization axis, as the propagation direction of electrons in a 1D system is fixed. However, this turns out to be correct only for a truly 1D electron system with vanishing width. In real quantum wires, such a situation is approximately realized when the spin-precession length² π/k_{so} is much larger than the wire width. Another way to formulate this condition is to say that the characteristic energy scale $\Delta_{so} = \hbar^2 k_{so}^2 / 2m$ for RSOC is small compared to the energy spacing of 1D subbands. For a quantum wire defined by a parabolic confining potential, e.g.,

$$V(x) = \frac{m}{2} \omega^2 x^2, \quad (2)$$

the latter would be $\hbar\omega$. When spin-orbit coupling is not small (i.e., when $\Delta_{so} \sim \hbar\omega$ for the case of parabolic confine-

ment), hybridization of 1D subbands for opposite spins becomes important, resulting in the deformation of electronic dispersion relations.¹¹ The effect of this deformation on transport properties has been the subject of recent investigation,¹¹ e.g., with respect to implications for the modulation of spin-polarized conductances as a function of RSOC strength¹² which is the principle of operation for spin-controlled field-effect devices.^{2,3}

Here we present results for the detailed spin structure of electron states in a quantum wire, defined by the parabolic confining potential $V(x)$ given in Eq. (2), with strong RSOC present. Contrary to previous¹³ assumptions that were uncritically adopted in the recent literature,¹⁴ we find that electrons with large wave vectors in the lowest spin-split subbands have essentially parallel spin. The spin state that right-moving electrons converge toward is opposite to that for left movers. This counterintuitive result will be explained qualitatively in the following paragraph, before presenting analytical and numerical results for electronic dispersion curves and spin structure of eigenstates. A texturelike variation of spin density across the wire is identified. We then apply the Landauer-Büttiker formalism^{15,16} to discuss spin-dependent transport in hybrid systems of a wire with RSOC attached to leads where $k_{so} = 0$. Current turns out to be spin polarized in the wire but unpolarized in the leads. We elucidate the peculiar current conversion at wire-lead interfaces that sustains this novel type of spin accumulation in the wire. Finally, consequences for the low-energy description of interacting wires in terms of Tomonaga-Luttinger-type models are discussed.

We start by considering basic features for eigenstates of the Hamiltonian $H_{1D} = H_{2D} + V(x)$ which are 1D plane waves in the y coordinate with wave number k_y but bound in the x direction. At finite k_{so} , spin degeneracy is preserved only for eigenstates with $k_y = 0$; their energies are the shifted harmonic-oscillator levels $E_n^{(0)} = (\hbar\omega/2)(2n+1) - \Delta_{so}$. This result is exact. To characterize states with finite k_y , we rewrite $H_{1D} = H_{pb} + H_{mix}$ where

$$H_{pb} = \frac{p_x^2}{2m} + \frac{m\omega^2 x^2}{2} + \frac{\hbar^2 k_y^2}{2m} + \frac{\hbar^2 k_{so} k_y}{m} \sigma_x, \quad (3)$$

and $H_{mix} = -\hbar k_{so} \sigma_y p_x / m$. Straightforward calculation yields eigenstates of H_{pb} which are also eigenstates of σ_x

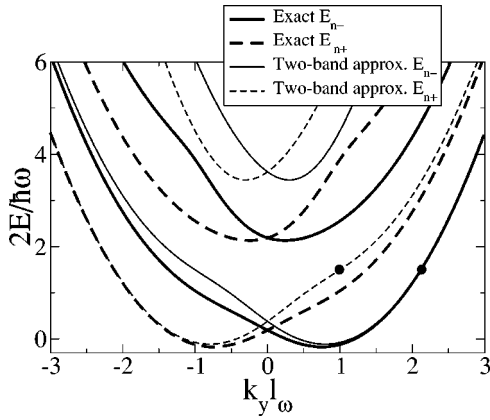


FIG. 1. Lowest and first-excited spin-split subbands of a quantum wire, defined by a parabolic confining potential with oscillator length l_ω in a 2D electron system, with strong Rashba spin-orbit coupling such that $k_{so}l_\omega=0.9$. Thick curves are results of the exact numerical calculation, while thin curves are obtained using the approximate two-band model which includes only spin-orbit-induced mixing of the lowest two parabolic subbands. Evidently, this approximation gives reasonable results for the lowest spin-split subband, even in the present case of a rather large spin-orbit coupling strength.

with eigenvalue $\sigma = \pm 1$ and have energies $E_{n\sigma}^{(pb)}(k_y) = (\hbar\omega/2)(2n+1) + (\hbar^2/2m)(k_y + \sigma k_{so})^2 - \Delta_{so}$. The term H_{mix} induces mixing between the shifted parabolic subbands $E_{n\sigma}^{(pb)}(k_y)$. To lowest order in perturbation theory, it results in a uniform shift of eigenenergies by $-\Delta_{so}$ and a small deviation of spin quantization in x direction.¹⁷ Hence, for $\Delta_{so} \ll \hbar\omega$, eigenstates of H_{1D} have energies $E_{n\sigma}^{(pb)}(k_y) - \Delta_{so}$ and are, to a good approximation, eigenstates of σ_x . When Δ_{so} becomes comparable to the subband splitting, anticrossings occur between neighboring subbands with *opposite* spin index σ . As a result, no common spin-quantization axis can be defined anymore for eigenstates within any subband. Far enough from anticrossings, eigenstates of H_{1D} will essentially be eigenstates of H_{pb} . In particular, their spins will be approximately aligned in the x direction. In the lowest two subbands, right movers with wave vectors larger than that of the anticrossing point can then have approximately parallel spin. The same is true for left movers whose asymptotic spin direction is opposite to that of right-movers.

In Fig. 1, we show as thick lines numerically calculated spectra of H_{1D} for a large value of spin-orbit coupling. Deviation from parabolicity is clearly visible. Interestingly, it is possible to obtain a good quantitative description of the lowest spin-split subband by diagonalizing H_{1D} in a truncated Hilbert space which is spanned by the lowest and first-excited spin-degenerate parabolic subbands of the Hamiltonian $H_0 + V(x)$. We call this the *two-band* model and find an approximate expression for the dispersion of the lowest spin-split subband,

$$\frac{2E_{0\gamma}^{(2b)}}{\hbar\omega} = 2 + (k_y l_\omega)^2 - \sqrt{(1 - \gamma 2k_{so}k_y l_\omega^2)^2 + 2(k_{so}l_\omega)^2}, \quad (4)$$

where $l_\omega = \sqrt{\hbar/m\omega}$ is the oscillator length of the parabolic confinement and $\gamma = \pm$ a subband index that does *not* have the meaning of a spin-quantization number. We show Eq. (4) and the corresponding result for the first-excited subband as thin lines in Fig. 1. It is seen that the two-band model is quite adequate for the lowest subbands, even for rather strong spin-orbit coupling.

Results shown in Fig. 2 confirm conclusions reached in our previous discussion of the spin structure of electron eigenstates with RSOC present. Panel (a) shows the expectation value of spin component in the x direction for eigenstates of H_{1D} in the lowest and first excited spin-split subbands for the same value of k_{so} used in Fig. 1. Data in Figs. 1 and 2 for the same subband are indicated by the same line type. For the lowest subbands, we also give, as thin lines, results obtained analytically within the two-band model. It is clearly seen that spins of eigenstates with large absolute value of wave number are approximately quantized in the x direction, with the spin direction of left movers being opposite to that of right movers.²⁷ This fact is underscored by the properties of the energy spectrum in a finite magnetic field B in the x direction which is shown in panel (b). Clearly, the Zeeman shift of states at large positive wave number is opposite to that for states with large negative wave number. Shown as thin lines in the main figure of panel (a) are curves obtained analytically within the two-band model which yields again reliable results for the lowest subbands. We therefore use it to calculate the variation of spin density $\vec{s}(x) = \Phi^\dagger(x)\vec{\sigma}\Phi(x)$ across the wire. [The spinor $\Phi(x)$ denotes the transverse part of an eigenfunction of H_{1D} which, in the presence of spin-orbit coupling, depends on wave vector.] It turns out that the density $s_y(x)$ of spin components parallel to the wire vanishes identically. Hence, only the x and z components of the spin density are shown in Fig. 3, displaying an interesting texturelike variation with coordinate x whose structure reflects the mixing between subbands due to H_{mix} . Note that the *expectation value* for the z component of spin vanishes for eigenstates of H_{1D} .

From the above it has become clear that, in general, spin quantum number is *not* an appropriate way to characterize electron states in a quantum wire with strong RSOC. Only states with wave number k_y far enough from anticrossing points will asymptotically have their spin quantized in the x direction. From considering Figs. 1 and 2, the following special situation can be envisioned which has rather counterintuitive consequences. At low enough electron density such that only states in the lowest spin-split subbands are occupied, states near the Fermi energy ε_F will be localized near four Fermi points. When the electron density is not too low, their spins are approximately quantized in the x direction. As pointed out above, spins of states near Fermi points for right movers are approximately spin down, opposite to the spin direction of left-moving states near ε_F . Assuming it to be possible to selectively raise (lower) the electrochemical potential of right movers (left movers), a spin-polarized current could be generated. Usually, creating a population of left movers and right movers with different electrochemical potentials is achieved by coupling the quantum wire adiabati-

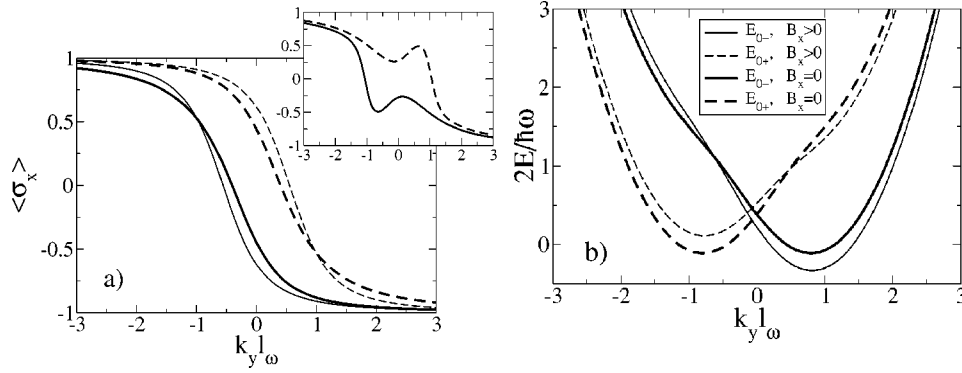


FIG. 2. Spin structure of electron states in a quantum wire with strong spin-orbit coupling. (a) Expectation value of spin projection onto the x direction for electron states obtained in Fig. 1. Results of exact numerical calculation for the lowest spin-split subbands (main figure) and first-excited spin-split subbands (inset) are given by thick curves. The effective two-band model reasonably approximates the behavior of the lowest subband (thin lines in the main figure). Right-moving electrons with large wave vectors asymptotically have parallel spin which is opposite to that of left movers. The same can be observed in (b) where the spectrum in a finite magnetic field B pointing in x direction is compared with that in zero field. Here dispersion curves are calculated within the two-band model for Zeeman energy $g\mu_B B = 0.25\hbar\omega$ (thin lines) and in zero magnetic field (thick lines).

cally to ideal contacts.^{15,16} However, the underlying assumption that excess electrons injected from the right (left) reservoir will only be spin up (spin down) is not realistic because, typically, RSOC will be absent in the contacts. The different nature of electron states in the wire and the leads will result in strong scattering at wire-lead interfaces. Similar to the approach taken in Ref. 12, we model this situation by attaching semi-infinite leads with $k_{so}=0$ to the wire where $k_{so} \neq 0$. The transmission problem can be solved exactly by matching appropriate *Ansätze* for wave functions in the wire

and the leads. The usual condition for ensuring current conservation has to be modified because the group velocity for electrons in the quantum wire with RSOC reads^{18,19}

$$v_y = \hbar(k_y + k_{so}\sigma_x)/m. \quad (5)$$

Despite the unusual spin structure at the four Fermi points which is asymmetric with respect to right movers and left movers, no spin-polarized current is generated *in the leads*. However, as is shown in Fig. 4, a process of current conversion occurs close to the interfaces in the wire that results in a *finite spin polarization of current in the wire*. We have therefore found a unique type of spin accumulation that is not, as in the usual case,²⁰ induced by ferromagnetic contacts. Our analysis shows that current conversion is enabled by scattering into evanescent modes of the wire because of the peculiar form of the velocity operator (5). A four-terminal measurement with ferromagnetic contacts as weakly coupled voltage probes should enable experimental verification of spin accumulation in the wire.

Finally, we briefly remark on the effective low-energy description of an interacting quantum wire with strong RSOC. In the spirit of Tomonaga-Luttinger models^{21,22} for interacting 1D systems, we linearize the single-electron energy spectrum close to the four Fermi points. We explicitly avoid attaching any spin labels. Rather, we define type-A (type-B) right movers and left movers having *the same* velocity v_A (v_B). Typical electron-electron interactions give rise to a term $H_{int} = \frac{1}{2} \int_{x',y'}^{x,y} \psi^\dagger \psi(x,y) U(x-x', y-y') \psi^\dagger \psi(x',y')$ in the electron Hamiltonian. In the low-energy, long-wave length limit, we can write $\psi(x,y) = \sum_{\beta=R,L}^{\alpha=A,B} \psi_{\alpha\beta}(y) \Phi_{k_{F\alpha\beta}}(x)$ and assume U to be long range on the scale of the wire width but short range on the scale of the wire length. It is important to note that the present case differs from the usual one in that the transverse wave-function spinors $\Phi_{k_{F\alpha\beta}}(x)$ are *nearly orthogonal*. As a result, backscattering processes are strongly suppressed. Apart from this fact and the peculiar spin struc-

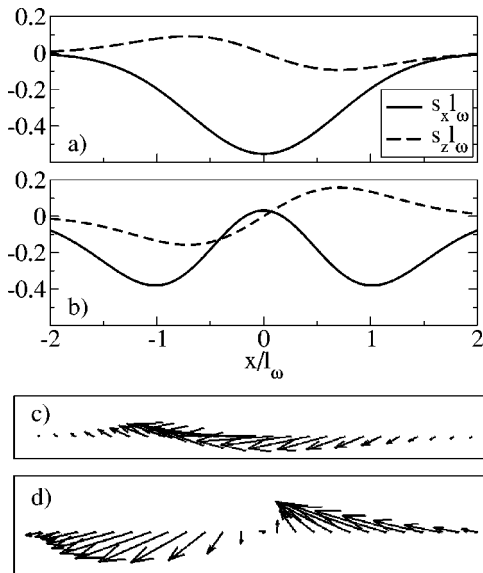


FIG. 3. Texturelike structure of spin density across the quantum wire, calculated within the two-band model for states indicated by black dots in Fig. 1, which have energy $0.75\hbar\omega$. (a) Spatial variation of nonzero components of spin density for the state with larger wave vector. (b) Same for the other state. (c) Visualization of spin texture for the same state as (a). Arrow length is proportional to spin density. (d) Spin texture visualized for the same state as considered in (b).

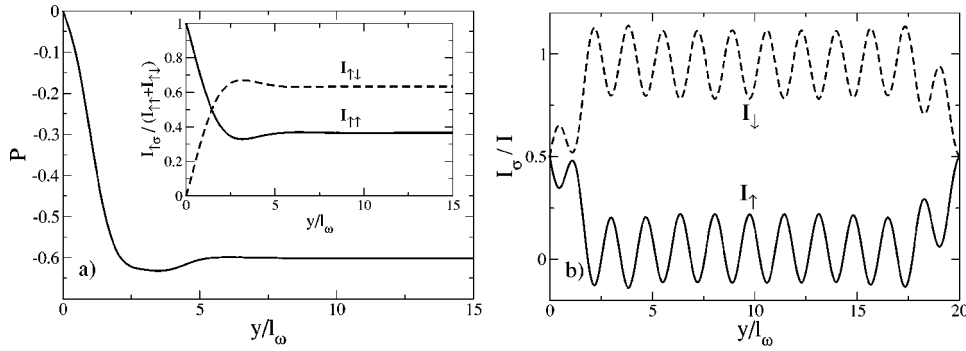


FIG. 4. Transport in hybrid systems of a wire with strong Rashba spin-orbit coupling and ideal leads, calculated exactly using the Landauer–Büttiker formalism within the two-band model (inclusion of higher subbands leads only to small quantitative changes). Panel a) shows the spatial variation of current polarization in a semi-infinite wire ($y > 0$) attached to an ideal lead ($y < 0$). Conversion of incident spin-up current is illustrated in the inset. Here $I_{\sigma\uparrow}$ denotes the spin- σ current in the wire when spin- \uparrow current is injected from the lead. A finite spin polarization exists also in a finite wire with to semi-infinite leads attached [panel b)]. Here quantum interference gives rise to additional oscillatory structure. Parameters used in the calculation are $E_F = 1 \hbar \omega$ and $k_{so} = 0.9 l_\omega^{-1}$.

ture of states near the four Fermi points, the present system is identical, on a formal level, to a two-component²³ or Zeeman-split²⁴ Tomonaga-Luttinger model. The response to an external magnetic field will, however, be special in the present case. Postponing a detailed analysis to a later publication, we mention here only a few basic facts. When Fermi points are far enough away from anticrossings, a magnetic field B applied in x direction will shift right movers (left movers) to higher (lower) energies. [See Fig. 2(b).] The Zeeman term in bosonized form reads then $H_Z = (-\Delta_Z / \sqrt{2\pi}) \int_x \Pi_\rho$, where Π_ρ is canonically conjugate to

the phase field θ_ρ that is related, within the usual²⁵ phase-field formalism, to the total electron density $\rho_{tot} = \sum_{\beta=R,L} \rho_{\alpha\beta}$ via $\sqrt{2/\pi} \partial_y \theta(y) = \rho_{tot}(y)$. Approximate orthogonality of transverse parts of electron wave functions enables spin-flip processes, in the long-wave-length limit, only between left-moving and right-moving branches of the same type (A or B). In general, any spin-flip process incurs a large momentum transfer.

This work was supported by the DFG Center for Functional Nanostructures at the University of Karlsruhe.

¹S.A. Wolf *et al.*, Science **294**, 1488 (2001).

²S. Datta and B. Das, Appl. Phys. Lett. **56**, 665 (1990).

³J. Nitta, F.E. Meijer, and H. Takayanagi, Appl. Phys. Lett. **75**, 695 (1999).

⁴E.I. Rashba, Fiz. Tverd. Tela (Leningrad) **2** 1224 (1960), [Sov. Phys. Solid State **2**, 1109 (1960)].

⁵G. Lommer, F. Malcher, and U. Rössler, Phys. Rev. Lett. **60**, 728 (1988).

⁶R. Winkler, Phys. Rev. B **62**, 4245 (2000).

⁷Y.A. Bychkov and E.I. Rashba, J. Phys. C **17**, 6039 (1984).

⁸J. Nitta, T. Akazaki, H. Takayanagi, and T. Enoki, Phys. Rev. Lett. **78**, 1335 (1997).

⁹T. Schäpers *et al.*, J. Appl. Phys. **83**, 4324 (1998).

¹⁰D. Grundler, Phys. Rev. Lett. **84**, 6074 (2000).

¹¹A.V. Moroz and C.H.W. Barnes, Phys. Rev. B **60**, 14272 (1999).

¹²F. Mireles and G. Kirczenow, Phys. Rev. B **64**, 024426 (2001).

¹³A.V. Moroz, K.V. Samokhin, and C.H.W. Barnes, Phys. Rev. Lett. **84**, 4164 (2000).

¹⁴A. De Martino and R. Egger, Europhys. Lett. **56**, 570 (2001).

¹⁵R. Landauer, IBM J. Res. Dev. **1**, 223 (1957).

¹⁶M. Büttiker, IBM J. Res. Dev. **32**, 317 (1988).

¹⁷W. Häusler, Phys. Rev. B **63**, 121310 (2001).

¹⁸L.W. Molenkamp, G. Schmidt, and G.E.W. Bauer, Phys. Rev. B **64**, 121202(R) (2001).

¹⁹U. Zülicke and C. Schroll, Phys. Rev. Lett. **88**, 029701 (2002).

²⁰P.C. van Son *et al.*, Phys. Rev. Lett. **58**, 2271 (1987).

²¹S. Tomonaga, Prog. Theor. Phys. **5**, 544 (1950).

²²J.M. Luttinger, J. Math. Phys. **4**, 1154 (1963).

²³K. Penc and J. Sólyom, Phys. Rev. B **47**, 6273 (1993).

²⁴T. Kimura, K. Kuroki, and H. Aoki, Phys. Rev. B **53**, 9572 (1996).

²⁵J. Voit, Rep. Prog. Phys. **57**, 977 (1994).

²⁶Band nonparabolicity typically plays no role in the low-density quantum wires considered here.

²⁷This result contradicts the spin labeling of subbands adopted in Refs. 13 and 14.